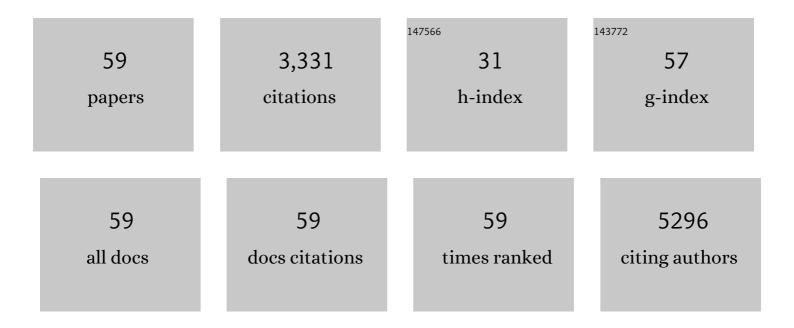
## Hung-We I Yang

List of Publications by Year in descending order

Source: https://exaly.com/author-pdf/6433517/publications.pdf Version: 2024-02-01



HUNC-WELYANC

#	Article	IF	CITATIONS
1	Design the RNA aptamer of PCA3 long non-coding ribonucleic acid by the coarse-grained molecular mechanics. Journal of Biomolecular Structure and Dynamics, 2022, 40, 13833-13847.	2.0	1
2	Sodium Thiosulfate Improves Hypertension in Rats with Adenine-Induced Chronic Kidney Disease. Antioxidants, 2022, 11, 147.	2.2	9
3	Microneedle patches integrated with lateral flow cassettes for blood-free chronic kidney disease point-of-care testing during a pandemic. Biosensors and Bioelectronics, 2022, 208, 114234.	5.3	8
4	Melatonin Prevents Chronic Kidney Disease-Induced Hypertension in Young Rat Treated with Adenine: Implications of Gut Microbiota-Derived Metabolites. Antioxidants, 2021, 10, 1211.	2.2	10
5	Rapid Detection of Gut Microbial Metabolite Trimethylamine N-Oxide for Chronic Kidney Disease Prevention. Biosensors, 2021, 11, 339.	2.3	16
6	Glucose/Glutathione Co-triggered Tumor Hypoxia Relief and Chemodynamic Therapy to Enhance Photothermal Therapy in Bladder Cancer. ACS Applied Bio Materials, 2021, 4, 7485-7496.	2.3	12
7	A serological point-of-care test for Zika virus detection and infection surveillance using an enzyme-free vial immunosensor with a smartphone. Biosensors and Bioelectronics, 2020, 151, 111960.	5.3	31
8	Maternal Adenine-Induced Chronic Kidney Disease Programs Hypertension in Adult Male Rat Offspring: Implications of Nitric Oxide and Gut Microbiome Derived Metabolites. International Journal of Molecular Sciences, 2020, 21, 7237.	1.8	35
9	Mechanism of Nanoformulated Graphene Oxide-Mediated Human Neutrophil Activation. ACS Applied Materials & Interfaces, 2020, 12, 40141-40152.	4.0	18
10	Perinatal Resveratrol Therapy Prevents Hypertension Programmed by Maternal Chronic Kidney Disease in Adult Male Offspring: Implications of the Gut Microbiome and Their Metabolites. Biomedicines, 2020, 8, 567.	1.4	31
11	A new lateral flow plasmonic biosensor based on gold-viral biomineralized nanozyme for on-site intracellular glutathione detection to evaluate drug-resistance level. Biosensors and Bioelectronics, 2020, 165, 112325.	5.3	27
12	Instrument-Free Detection of FXYD3 Using Vial-Based Immunosensor for Earlier and Faster Urothelial Carcinoma Diagnosis. ACS Sensors, 2020, 5, 928-935.	4.0	6
13	Mobile healthcare system based on the combination of a lateral flow pad and smartphone for rapid detection of uric acid in whole blood. Biosensors and Bioelectronics, 2020, 164, 112309.	5.3	35
14	On-skin glucose-biosensing and on-demand insulin-zinc hexamers delivery using microneedles for syringe-free diabetes management. Chemical Engineering Journal, 2020, 398, 125536.	6.6	34
15	Combined Detection of CA19–9 and MUC1 Using a Colorimetric Immunosensor Based on Magnetic Gold Nanorods for Ultrasensitive Risk Assessment of Pancreatic Cancer. ACS Applied Bio Materials, 2019, 2, 4847-4855.	2.3	18
16	Ovalbumin-Loaded Gelation Microneedles Made of Predictive Formulation by Molecular Dynamics Simulation for Enhancement of Skin Immunization. ACS Biomaterials Science and Engineering, 2019, 5, 6012-6021.	2.6	3
17	Predicting the Most Stable Aptamer/Target Molecule Complex Configuration Using a Stochastic-Tunnelling Basin-Hopping Discrete Molecular Dynamics Method: A Novel Global Minimum Search Method for a Biomolecule Complex. Computational and Structural Biotechnology Journal, 2019, 17, 812-820.	1.9	6
18	Direct glucose detection in whole blood by colorimetric assay based on glucose oxidase-conjugated graphene oxide/MnO <sub>2</sub> nanozymes. Analyst, The, 2019, 144, 3038-3044.	1.7	58

HUNG-WE I YANG

#	Article	IF	CITATIONS
19	Bioengineering fluorescent virus-like particle/RNAi nanocomplexes act synergistically with temozolomide to eradicate brain tumors. Nanoscale, 2019, 11, 8102-8109.	2.8	31
20	Convection-Enhanced Delivery of a Virus-Like Nanotherapeutic Agent with Dual-Modal Imaging for Besiegement and Eradication of Brain Tumors. Theranostics, 2019, 9, 1752-1763.	4.6	43
21	A colorimetric immunosensor based on self-linkable dual-nanozyme for ultrasensitive bladder cancer diagnosis and prognosis monitoring. Biosensors and Bioelectronics, 2019, 126, 581-589.	5.3	52
22	Image-Guided Focused-Ultrasound CNS Molecular Delivery: An Implementation via Dynamic Contrast-Enhanced Magnetic-Resonance Imaging. Scientific Reports, 2018, 8, 4151.	1.6	14
23	Diagnosis by simplicity: an aptachip for dopamine capture and accurate detection with a dual colorimetric and fluorometric system. Journal of Materials Chemistry B, 2018, 6, 3387-3394.	2.9	13
24	Aptasensor designed via the stochastic tunneling-basin hopping method for biosensing of vascular endothelial growth factor. Biosensors and Bioelectronics, 2018, 119, 25-33.	5.3	15
25	An electrochemical biosensor to simultaneously detect VEGF and PSA for early prostate cancer diagnosis based on graphene oxide/ssDNA/PLLA nanoparticles. Biosensors and Bioelectronics, 2017, 89, 598-605.	5.3	193
26	Coâ€Delivery of Docetaxel and p44/42 MAPK siRNA Using PSMA Antibodyâ€Conjugated BSAâ€PEI Layerâ€by‣ Nanoparticles for Prostate Cancer Target Therapy. Macromolecular Bioscience, 2017, 17, 1600421.	ayer 2.1	24
27	Ebola Vaccination Using a DNA Vaccine Coated on PLGAâ€PLL/γPGA Nanoparticles Administered Using a Microneedle Patch. Advanced Healthcare Materials, 2017, 6, 1600750.	3.9	92
28	Functional RNAs: combined assembly and packaging in VLPs. Nucleic Acids Research, 2017, 45, 3519-3527.	6.5	37
29	Rapid <i>In Situ</i> MRI Traceable Gel-forming Dual-drug Delivery for Synergistic Therapy of Brain Tumor. Theranostics, 2017, 7, 2524-2536.	4.6	21
30	Label-Free Biochips for Accurate Detection of Prostate Cancer in the Clinic: Dual Biomarkers and Circulating Tumor Cells. Theranostics, 2017, 7, 4289-4300.	4.6	15
31	Self-Assembly DNA Polyplex Vaccine inside Dissolving Microneedles for High-Potency Intradermal Vaccination. Theranostics, 2017, 7, 2593-2605.	4.6	39
32	1,3-Bis(2-chloroethyl)-1-nitrosourea-loaded bovine serum albumin nanoparticles with dual magnetic resonance–fluorescence imaging for tracking of chemotherapeutic agents. International Journal of Nanomedicine, 2016, Volume 11, 4065-4075.	3.3	9
33	Fabrication of a Nanogold-Dot Array for Rapid and Sensitive Detection of Vascular Endothelial Growth Factor in Human Serum. ACS Applied Materials & Interfaces, 2016, 8, 30845-30852.	4.0	19
34	Non-invasive screening for early Alzheimer's disease diagnosis by a sensitively immunomagnetic biosensor. Scientific Reports, 2016, 6, 25155.	1.6	55
35	A reusable magnetic graphene oxide-modified biosensor for vascular endothelial growth factor detection in cancer diagnosis. Biosensors and Bioelectronics, 2015, 67, 431-437.	5.3	103
36	Biodistribution of PEGylated graphene oxide nanoribbons and their application in cancer chemo-photothermal therapy. Carbon, 2014, 74, 83-95.	5.4	69

HUNG-WE I YANG

#	Article	IF	CITATIONS
37	Combined Detection of Cancer Cells and a Tumor Biomarker using an Immunomagnetic Sensor for the Improvement of Prostate ancer Diagnosis. Advanced Materials, 2014, 26, 3662-3666.	11.1	39
38	Magnetic-Composite-Modified Polycrystalline Silicon Nanowire Field-Effect Transistor for Vascular Endothelial Growth Factor Detection and Cancer Diagnosis. Analytical Chemistry, 2014, 86, 9443-9450.	3.2	18
39	Gadolinium-functionalized nanographene oxide for combined drug and microRNA delivery and magnetic resonance imaging. Biomaterials, 2014, 35, 6534-6542.	5.7	152
40	Nonâ€Invasive Synergistic Treatment of Brain Tumors by Targeted Chemotherapeutic Delivery and Amplified Focused Ultrasoundâ€Hyperthermia Using Magnetic Nanographene Oxide. Advanced Materials, 2013, 25, 3605-3611.	11.1	83
41	Magnetic gold-nanorod/ PNIPAAmMA nanoparticles for dual magnetic resonance and photoacoustic imaging and targeted photothermal therapy. Biomaterials, 2013, 34, 5651-5660.	5.7	123
42	EGRF conjugated PEGylated nanographene oxide for targeted chemotherapy and photothermal therapy. Biomaterials, 2013, 34, 7204-7214.	5.7	133
43	Reusable sensor based on high magnetization carboxyl-modified graphene oxide with intrinsic hydrogen peroxide catalytic activity for hydrogen peroxide and glucose detection. Biosensors and Bioelectronics, 2013, 41, 172-179.	5.3	61
44	Enhanced therapeutic agent delivery through magnetic resonance imaging–monitored focused ultrasound blood-brain barrier disruption for brain tumor treatment: an overview of the current preclinical status. Neurosurgical Focus, 2012, 32, E4.	1.0	34
45	Improving thermal stability and efficacy of BCNU in treating glioma cells using PAA-functionalized graphene oxide. International Journal of Nanomedicine, 2012, 7, 1737.	3.3	53
46	Preparation of water-dispersible poly[aniline-co-sodium N-(1-one-butyric acid) aniline]–zinc oxide nanocomposite for utilization in an electrochemical sensor. Journal of Materials Chemistry, 2012, 22, 13252.	6.7	10
47	Cooperative Dual-Activity Targeted Nanomedicine for Specific and Effective Prostate Cancer Therapy. ACS Nano, 2012, 6, 1795-1805.	7.3	54
48	Bioconjugation of recombinant tissue plasminogen activator to magnetic nanocarriers for targeted thrombolysis. International Journal of Nanomedicine, 2012, 7, 5159.	3.3	41
49	Potential of magnetic nanoparticles for targeted drug delivery. Nanotechnology, Science and Applications, 2012, 5, 73.	4.6	64
50	Manipulation of magnetic nanoparticle retention and hemodynamic consequences in microcirculation: assessment by laser speckle imaging. International Journal of Nanomedicine, 2012, 7, 2817.	3.3	4
51	An epirubicin–conjugated nanocarrier with MRI function to overcome lethal multidrug-resistant bladder cancer. Biomaterials, 2012, 33, 3919-3930.	5.7	23
52	Superhigh-magnetization nanocarrier as a doxorubicin delivery platform for magnetic targeting therapy. Biomaterials, 2011, 32, 8999-9010.	5.7	80
53	In vivo MR quantification of superparamagnetic iron oxide nanoparticle leakage during Iowâ€frequencyâ€ultrasoundâ€induced blood–brain barrier opening in swine. Journal of Magnetic Resonance Imaging, 2011, 34, 1313-1324.	1.9	27
54	The effectiveness of a magnetic nanoparticle-based delivery system for BCNU in the treatment of gliomas. Biomaterials, 2011, 32, 516-527.	5.7	142

HUNG-WE I YANG

#	Article	IF	CITATIONS
55	Self-protecting core-shell magnetic nanoparticles for targeted, traceable, long half-life delivery of BCNU to gliomas. Biomaterials, 2011, 32, 6523-6532.	5.7	70
56	Magnetic-nanoparticle-modified paclitaxel for targeted therapy for prostate cancer. Biomaterials, 2010, 31, 7355-7363.	5.7	115
57	Blood-Brain Barrier Disruption with Focused Ultrasound Enhances Delivery of Chemotherapeutic Drugs for Glioblastoma Treatment. Radiology, 2010, 255, 415-425.	3.6	337
58	Novel magnetic/ultrasound focusing system enhances nanoparticle drug delivery for glioma treatment. Neuro-Oncology, 2010, 12, 1050-1060.	0.6	115
59	Magnetic resonance monitoring of focused ultrasound/magnetic nanoparticle targeting delivery of therapeutic agents to the brain. Proceedings of the National Academy of Sciences of the United States of America, 2010, 107, 15205-15210.	3.3	351